

Flow Science Report 05-14

Moisture Drying Model

Flow Science, Inc.

C.W. Hirt

October 2014

Introduction

In the manufacture of paper it is necessary to remove all water from the paper before it is rolled up. The majority of water is typically removed by squeezing the paper between large rollers. The remaining moisture can be removed by forcing hot air through the paper to accelerate its evaporation.

Using heated air can be an expensive process so there is interest in investigating optimum arrangements for achieving the fastest and least expensive means of removing the residual water from paper. A prototype arrangement using heated air is shown in the following figure:

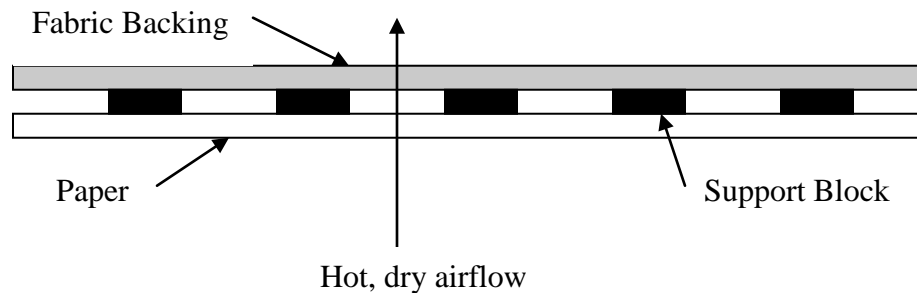


Figure 1. Schematic of paper drying process

Both the paper and the fabric backing are porous materials. The support blocks may not be porous. It is expected that the permeability of the fabric and paper will be a function of their water content.

This report describes a software development that allows for a realistic treatment of the drying process in porous media such as that shown in Fig. 1. A description is given of the new model, which has been validated with available data. This data does not cover the entire range of moisture content or airflow rates that are typically encountered in practice. Consequently, it may be found necessary to make some small model adjustments. It is hoped that the formulation of the model, which is based on simple physical principles, will be easy to adjust to fit a larger range of observations.

Before describing the new model, a better perspective of its capabilities can be appreciated by noting some of the ways that it differs from previous work on paper

drying. Most importantly, the new model considers the paper as having finite thickness and properties such as moisture content, temperature and vapor concentration that vary through the thickness. Thus, the paper may have dried on the upstream side, but still be completely wet on the opposite side. Another difference is that air and water vapor constitute a two-component gas that is compressible. Compressibility means, for example, that the gas velocity in the paper must increase in the direction of flow because of the decrease in pressure through the paper (i.e., density and/or temperature must decrease by expansion to give a pressure decrease). Since flow velocity has an important effect on drying rate, compressibility can influence local drying conditions in the paper. Finally, by computing transient conditions throughout the paper, this model could be used to investigate arbitrary non-uniform initial conditions or paper with a non-uniform thickness and/or porosity distribution.

Model and Basic Assumptions

The new model is to be used in connection with the *FLOW-3D*¹ computational fluid dynamics software. Although it is a fully three-dimensional and time-dependent model it can be just as easily used for two-dimensional arrangements such as that shown in the prototype figure.

Porosity Assumption

It is assumed that water in a porous material directly contributes to a lowering of the porosity of the paper material. Because of this, water also alters the permeability of the paper and can thereby affect the airflow rate passing through it. As the moisture content of the paper is reduced its permeability increases, which means the model accounts for a time-dependent porosity.

Wicking Assumption

Although variable moisture content is allowed because of evaporation, we have not accounted for wicking of liquid in the paper. This assumption resulted in a large savings in model development since it was possible to use an existing capability in *FLOW-3D* for placing water in a porous medium. The existing “moisture model” was intended to represent water in sand molds used for metal casting. When a mold is heated by liquid metal it is able to absorb more heat and remain at a lower temperature because of its water content. The new model uses all the same input and control parameters for water initialization and evaporation that were available for the casting moisture model. Consequently, only a few additional code changes were required.

The main limitation of the original casting moisture model is that it does not contain any provision for the wicking of water in porous material, nor will high-speed airflow be able to displace any water. In most cases air-driven water movement is not likely to be a problem since water in the paper will be tightly attached by surface tension to the fiber matrix making up the paper. In any case, adding a wicking capability would require considerable additional model development, so it has been ignored in the present model.

Temperature Assumption

¹ *FLOW-3D* and *TruVOF* are registered trademarks in the US and other countries.

Another assumption made is that the temperature of the water is equal to the temperature of the solid content in the paper. This assumption is unlikely to have much of an effect on the outcome of the simulations. The water and porous material are in close contact and distributed on a scale that is fine compared to the thickness of the paper, which means that heat conduction in these materials should relatively quickly equilibrate their local temperatures.

Basic Model Description

All geometric features can be initialized with the standard *FLOW-3D* program; the fabric and paper are defined as porous components of given porosity and the support blocks are solid components. A support structure consisting of a screen could be modeled using the baffle capability in the program, provided it remains aligned with a grid plane.

Thermal properties must be defined for all the solids, including initial temperature, density, specific heat, heat-conduction coefficient and heat-transfer coefficient between solid and gas.

The water initially in the porous material is defined by a set of component properties that include water volume fraction, heat capacity and latent heat. The new model has a full non-equilibrium phase-change capability. Initialization of moisture in a component is uniform in the component. A simple non-uniform distribution could be defined by using multiple components each with a different water content. More general distributions could be implemented, but would require further development effort.

A single, compressible fluid model, with no free surfaces, is necessary for modeling the flow of gas (i.e., air and vapor). Pressure boundaries can be used on either side of the paper assembly to generate the airflow or a flow rate can be specified at one side.

An important component of the model is the heat transfer between gas and paper (i.e., solids plus water). Surface area per unit volume in the porous material is an input quantity and is used for heat transfer and phase change. This quantity can be estimated in terms of an average diameter of water particles in the paper (or the diameter of the fibers). A typical value for the surface area per unit volume, if the particles are assumed to be spherical, is

$$A_s = 6 * F_w / d_w,$$

where F_w is the volume fraction of water (or alternately, solids F_s) and d_w is the average diameter of the water particles in the paper (or alternately, fiber diameter d_f). A more correct expression in the case of fibers is to replace the factor of 6 by 4 because the fibers are more like rods than spheres. The surface area of the fibers is generally quite large because they consist of a great many fibers of small diameter. On the other hand, water has a smaller surface area because surface tension always tries to seek the smallest area possible.

As a first guess we have assumed that the water drops try to fit in between the fibers, or that the ratio of scale sizes is equal to the ratio of open to blocked volume fractions,

$$\frac{d_w}{d_f} = \frac{1 - F_s}{F_s}.$$

The water or fiber scale size is not presently an input parameter. It is up to the user to define input for the corresponding quantities OADRG, OBDRG for resistance to flow in the media (i.e. related to the reciprocal of permeability) and for OSPOR, the surface area per unit volume.

For most of the drying period it is the water scale size that is important, and it is assumed that the scale does not change during drying. This assumption could be relaxed if further validation studies indicate a need for such a refinement.

During the initial validation simulations, the heat-transfer coefficient between air and solid/water may need some adjustment to match experimental drying times. A simple approximation is that this coefficient should be equal to the minimum thermal conductivity in the gas and water/solid divided by a local length scale results in a value that seems much too large.

Developments for Drying Model

In discussing the basic model for paper drying several features were mentioned that involved assumptions or approximations. A summary of the developments and extensions that have been done to construct the new model is given here.

Flow Resistance

Flow resistance in the porous media must be adjusted for the water content, which can be thought of as contributing to flow blockage, i.e., a reduced porosity. For this we simply use the standard Reynolds number dependent, porous-media flow loss expression with its porosity reduced by the local water volume fraction. This formulation will automatically adjust to the porosity of dry paper as water is evaporated.

The size of the porous fibers, which is also used to compute drag coefficients, could also be adjusted to account for water content. This has not been done, however, because a review of data from Polat [1] for the viscous contribution to permeability shows that it varies with moisture content in a way that is reasonably well captured by the Kozeny-Carman equation. For example, Polat's Table 4.4 for a sheet basis weight of 50g/m² gives values for the viscous loss coefficient that vary with moisture content (by a factor of 7.6 for the range investigated). This variation is captured by the factor $(1-n)^2/n^2$ in the Kozeny-Carman[2] expression for the viscous coefficient, where n is the open volume fraction in the paper, $n=1-n_f-n_w$, in which the subscripts f and w refer to the volume fractions of fiber and liquid in the paper. Actually, the model variation in the viscous coefficient with moisture content is 6.8 versus 7.6 in the data. Although the correspondence is not perfect, with the limited data available it is recommended that the

Kozeny-Carman form of the Forchheimer [2] equation be accepted as a good first approximation.

The data of Polat has been used to set the fiber diameter size in the validation test problems described later. In particular, to agree with the viscous loss coefficient in the Forchheimer equation for dry paper, a fiber diameter of 0.0002cm was required.

Temperatures in Porous Media

The moisture model originally designed for sand molds uses a simple temperature adjustment to account for the added heat capacity of the water. It works as follows: a normal heat transfer computation is done between air and the solid parts of the porous material, ignoring the water. Then in the moisture-content sub-routine the heat added to the porous solid in a control element, which is computed in terms of its change in temperature, is redistributed over the sum of the solid and water content in the element to produce a corrected temperature for the combined solid and liquid content. Once this is done the evaporation routine determines how much water is evaporated and how much energy is lost in latent heat of evaporation.

A new phase-change routine has been written that is directly patterned after other phase-change models used in *FLOW-3D*. This model is based on a kinetic theory like rate process with a dependence on the local vapor saturation level in the air. The model has a non-dimensional coefficient referred to as an accommodation coefficient (*rsize* as used in all phase-change routines in the program for this purpose).

To use this model four input data are required. First, it is necessary to activate the model by defining *iphchg*=6. The accommodation coefficient, *rsize*, must be a positive, non-zero value and should be no greater than 1.0. A typical value for *rsize* is 0.05. It is also necessary to define a pressure-versus-temperature saturation relationship. The program uses a standard Clapeyron equation to define the saturation curve, which requires a temperature-pressure point (*pv1*, *tv1*) lying on the curve and an exponent value, *tvexp*. The exponent *tvexp* can be estimated from the relation $tvexp = (\gamma - 1) * cvvap / clhv1$, where γ is the ratio of specific heats for vapor, *cvvap* is the specific heat at constant volume for vapor and *clhv1* is the heat of vaporization.

Two-Component Gas Flow

In order to record and track water vapor through the paper drying apparatus it is necessary to use a two-component gas of air and vapor. This capability was recently added to *FLOW-3D* and appears in Version 9.3, where the air is referred to as a **non-condensable** gas (ng). To use this capability the program must be put into a two-fluid mode in which the second fluid is treated as a compressible gas. Compressibility will automatically adjust for newly vaporized or condensed water and the two-component feature will account for the mixed heat capacity of the air-vapor mixture.

Input for the two-component gas consists of a flag to activate the model, *incg*=1, and initial conditions (*cnci*) and boundary conditions (*cncbc*) to set the amount of non-

condensable gas in or entering the computational region. It is important to keep in mind that water vapor is the second fluid (gas) in the compressible, two-fluid model in *FLOW-3D* while air is the additional (non-condensable) component. This distinction must be remembered when entering property data into the input file.

Modeling Summary

With the exception of wicking during the drying process, the new paper-drying model addresses the major issues thought to influence the drying of paper by the through flow of dry air. The model has been built upon existing capabilities in *FLOW-3D* and adds features that account for flow resistance reduction as water is evaporated, a rate controlled phase change and the transport of water vapor with the airflow.

Validation of Model

To demonstrate the utility of the new paper-drying model at least two aspects of the paper drying process must be tested. One is the ability of the model to account for the effect of moisture content on permeability. The other is the drying rate for a given set of drying conditions.

Permeability of Paper

The first topic has already been partially addressed in the section “Developments for Drying Model,” subsection “Flow Resistance,” where it was observed that for low flow rates the primary flow resistance is one of viscous drag and that the often-used Kozeny-Carman model for porous media does a reasonable job of estimating the permeability. Some data obtained by Polat[1] were used for this purpose.

That same data also indicated that the second coefficient in the Forchheimer equation, relating to inertial flow resistance, was much more sensitive to moisture content than was the first coefficient. However, the measured pressure drop across the paper due to inertial effects was only on the order of 10% of the total pressure drop, even at the highest flow rate tested. This fact, coupled to the fact that the stated accuracy of the measurement were on the order of 7%, makes the estimates for the second coefficient suspect. The Kozeny-Carman type of permeability model, which works well for many kinds of porous media, does not correlate well with Polat’s data.

Certainly more testing is needed to clarify the dependence of permeability on moisture content, but this must wait until there is better data available.

Drying Rate Test Case

To check whether or not the new model can predict an accurate drying rate we have selected some data from a paper by Ryan et al. [3]. In particular, a specified flow rate case was chosen so that questions of permeability could be minimized. It should be noted that the authors of this paper also used data from Polat to help validate their experiments.

Unfortunately, not all of the experimental conditions were reported in the Ryan paper, but good guesses for most things could be made. The specific test selected was for a

relatively low air-flow rate at room temperature. These conditions are far from those used in many commercial paper drying operations, but they represent what is available.

The drying test results are given in Figure 7 of the paper by Ryan et al. [3], which shows, as a function of moisture content, the drying rate and temperature of the upstream surface of the paper. It is also stated in the text that the observed vapor exiting the paper is close to its saturated value. Drying time, pressure drop and several other quantities that would have been interesting to know are not given in the paper.

The selected drying test was for a sheet having basis weight 50 g/m^2 and 25% solids. A constant flow speed of 0.45 m/s was used with dry air having $0.0005 \text{ kg-water/kg-air}$. The initial moisture content of the paper was $3 \text{ kg-water/kg-fiber}$. Using these values and assuming a paper porosity of 0.9 and thickness of 0.25 mm (porosity and thickness were not specified) the density of the fiber is computed to be 490 kg/m^3 , which is close to that of pine or fir wood and confirms the choice of porosity and thickness as reasonable. The initial volume fraction of water is 0.147. A room temperature of 28.3°C (301.3°K) was used for an initial condition and for the incoming air. At $tv1=30^\circ\text{C}$ (303.0°K) the saturation pressure of water is $pv1=41950 \text{ dynes/cm}^2$. These values were used to initialize the vapor saturation curve ($pv1, tv1$) with $tvexp=2.0e-4$.

Approximately a 0.9 cm upstream region is modeled, as is a 0.3 cm region downstream of the paper. Specified flow conditions are fixed at the upstream boundary with a fixed pressure condition (room pressure and temperature) at the outlet of the computational region. The mesh consisted of 30 grid cells in the flow direction (6 cells covering the thickness of the paper) and 16 grid cells along the paper, perpendicular to the flow direction.

Upstream Boundary Conditions

An unanticipated problem arose with this setup, and illustrates how much one can learn from a computational simulation. In this case it was quickly discovered that the permeability of the paper is initially low enough to require an increase in the upstream pressure well above atmospheric (about 8%) in order to maintain the specified flow velocity through the paper. With an increase in pressure there is a corresponding increase in temperature because of gas compression. In other words, when the experimenters state that the inlet temperature is 301.3°K we cannot simply put this as the inlet boundary temperature. Furthermore, these upstream values change as drying progresses because the permeability increases and pressure decreases with the loss of moisture.

It can be assumed that the downstream condition is atmospheric pressure, while the upstream temperature was measured to be the 301.3°K value. Therefore, the simulation inlet boundary conditions were modified to have a pressure of $1.026e+6 \text{ dynes/cm}^2$ (atmospheric pressure is $1.0132e+6 \text{ dynes/cm}^2$), which is close to the expected value for dry paper. The inlet temperature was additionally reduced by 5 degrees to 296.3°K , which resulted in a value close to the measured 301.3°K at the paper at the start of the drying process. It is only when most of the moisture is gone that the inlet temperature at the paper surface approaches the specified temperature at the inlet boundary.

In retrospect, it is difficult to see how the Ryan experiment could have maintained a constant upstream temperature. The flow rate was specified using a choked flow device whose flow rate is not affected by downstream conditions. Also, it is not likely that the air temperature could have been controlled with this device to remain at a fixed value during the few seconds it took to dry the paper sample.

We interpret this finding as a positive result for the model; the numerical “experiment” has revealed some aspects of the experimental setup that were not anticipated.

Comparisons between Simulation and Experiment

Before looking at the details a quick view of the type of results obtained is given in Fig. 2, showing the distributions of velocity, pressure, moisture content and fiber/moisture temperature at a time of 1.0s. These plots include the entire region of the simulation.

The pressure drop across the paper is clearly indicated in Fig. 2a and the variation in moisture and temperature through the paper are obvious in the remaining two plots. A simulation time of about one hour was required on a single processor PC. Fluid advection limits the time-step size because of the small grid cells within the paper.

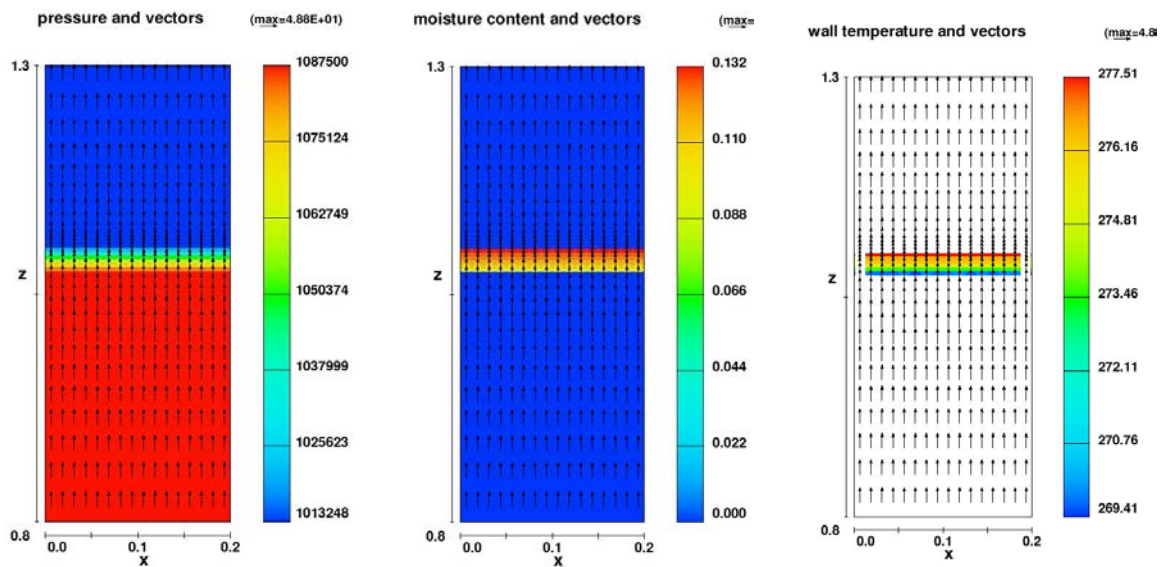


Figure 2a. Pressures and vectors at t=1.0s.

Figure 2b. Moisture content and vectors at t=1.0s.

Figure 2c. Temperature of paper and vectors at t=1.0s.

Simulations show that the reduction in moisture content in the paper proceeds progressively from the upstream to the downstream surface, Fig. 3. The first layer of paper is nearly dried while the last layer has only just started to dry out. There are two reasons for this rather sharp drying front; the air temperature is cooled by evaporation in the moisture it first encounters and the vapor generated quickly reaches saturation. Both of these things slow further evaporation downstream.

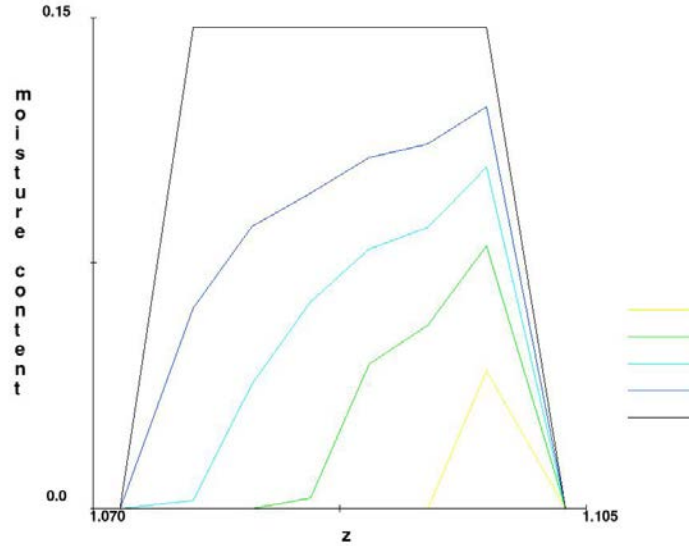


Figure 3. Moisture profiles through the paper at times 0, 2, 4, 6, 8 s. Total drying at 8.8s. Moisture content is volume fraction of moisture in the bulk porous media.

Ryan et al., report that the surface temperature of the paper (observed by an infrared detector) initially drops to the adiabatic saturation temperature and then rises continuously back to the inlet temperature. This also suggests that the air is rapidly being saturated with vapor. Simulation results show something slightly different and more interesting, Fig. 4. In the first layer of cells containing paper (at $t=1.0s$) the temperature of the gas is about $294.0K^\circ$ while the combined paper fiber and moisture are at a temperature of $273.0 K^\circ$. The pressure of vapor at this location is about $6842.0 \text{ dynes/cm}^2$, which is close to the saturation pressure based on the lower fiber/moisture temperature. This makes sense since the fiber/moisture cools rapidly as evaporation occurs due to the large heat of vaporization of the moisture. The gas temperature at this location has fallen from its inlet value but has not reached equilibrium with the fiber/moisture material. This leads one to ask just what temperature the infrared sensor was recording. Presumably it was some sort of average, and in fact the measured value is about $283.0 K^\circ$, right in the middle between the two temperatures of the simulation.

It may be noticed that the temperature histories have a stair-step appearance. This is typical of phase change problems when the heat of transformation is large compared to the internal energy of the fluids and heat conduction is significant. The steps arise from the numerical discretization. In this case the paper temperature is quite smooth until all the moisture in the cell has evaporated. Then a step appears because the paper temperature is no longer being cooled by evaporation and its temperature rises due to heating from the air. However, the next cell into the paper is now cooling by evaporation and conduction back to the surface cell holds its temperature down. The cooling lasts until all the moisture in the cell is evaporated, which is a finite amount associated with the size of the computational grid elements. This process proceeds through the paper, with each layer of cells affecting the surface cell, but by a small amount, as each layer is further away. There is currently no known solution to this numerical problem. Although the steps don't look good it must be remembered that the overall mass and energy

balances remain intact and the actual values should be a smoothed curve through the steps.

The simulated vapor pressure in the air downstream from the paper is close to its saturated value, Fig. 5, especially at early times when there is plenty of water in the paper. The saturation pressure in this case has been evaluated in terms of the gas temperature because there is no solid/moisture at this location. Within the paper the computed vapor pressure is much closer to the saturation value based on the solid/moisture temperature, as it should be.

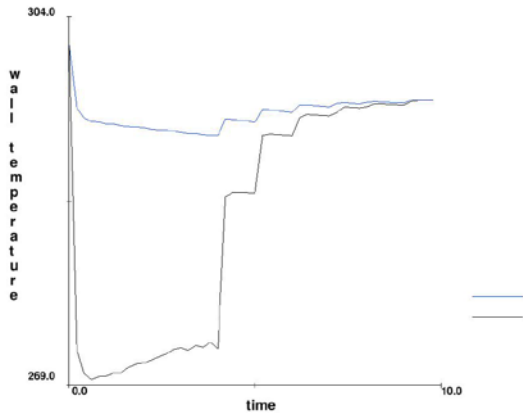


Figure 4. Paper (lower) and gas (upper) temperature histories at upstream surface.

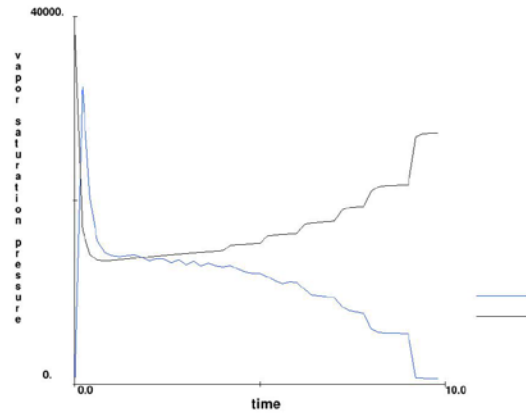


Figure 5. Vapor pressure (bottom curve) and saturation pressure (upper curve) at outlet

Finally, we compare the computed and measured drying rates. Figure 6 shows the history of total moisture content in the paper. After a short initialization the volume of moisture decreases nearly linearly, corresponding to a constant drying rate. Ryan et al., state that the observed rate is constant after the initial transient until the volume of moisture is reduced to a value of about 1.96 cc (0.8 kg-water/kg-fiber) after which the drying rate slows down. These observations are in agreement with the simulation results. Furthermore, the average drying rate, (total moisture)/(drying time), is computed to be $4.18e-4g/(cm^2s)$, which is in close agreement with the measure value (during the constant rate period) of $4.0e-4g/(cm^2s)$ or $14.4kg/(m^2h)$.

Additional Validation Test

The validation testing described in this paper was based on a paper drying example at room temperature and a relatively low flow rate (0.45m/s) of air compared to what is typical in industrial situations. In this test another example is presented for drying using air heated to 150°C and flow rates that exceed 2m/s. This example, referred to as the Weineisen case, is documented in “A Model for Through Drying of Tissue Paper at Constant Pressure Drop and High Drying Intensity,” by Henrik Weineisen and Stig Stenström, *DryingTech.* 25, 1949-1958 (2007).

This test case differs from the Ryan case in several ways. First, it uses a fixed pressure drop of 1.0 kPa across the paper and a fabric backing. The air is dry, but heated to 150°C.

The paper had a measured thickness of $210\mu\text{m}$ (0.0021cm) and a basis weight of $30\text{g}/\text{m}^2$ (moisture content of 3.0). The measured dry porosity was 0.91.

The authors quote a measured “pore size” distribution with a peak diameter of $21\mu\text{m}$. Pore size was used in the Weineisen paper as a characteristic of the structure of the paper, which they viewed as composed of a distribution of cylindrical channels. In the present case we have used the most probable pore diameter, $d_p = 21\mu\text{m}$, to estimate the surface area per unit volume, $ospor = 4(\text{volume fraction of moisture})/d_p = 204/\text{cm}$.

Determining the permeability of the paper/fabric is the most challenging element of the simulation. Weineisen and Stenström separate the pressure drops across the paper and fabric as acting in series. Across the fabric they use an empirical fit that is approximately proportional to the square of the flow velocity. In our simulation we have, therefore, chosen to represent the fabric backing by a baffle having the same porosity as the dry paper and a quadratic loss coefficient of 0.0346, which would give the Weineisen recommended loss if their expression were exactly quadratic.

The permeability of the paper was initially chosen to be the same as that used in the first validation test, however, this proved to be too small. With no other information we then decided to adjust the permeability to approximate the measured flow rate when the paper is dry (about 260 cm/s or $2.26\text{ kg-dry air}/\text{m}^2\text{s}$). Input for this limiting case was $oadrg = 9.18\text{e}+8$, $obdrg = 4548.0$ corresponding to a solid fiber diameter of 0.00044cm .

The general simulation setup was the same as that used for the Ryan case, with small changes to fit the paper thickness, the addition of the fabric “baffle,” and slightly different porosity, permeability and initial/boundary conditions.

The experimental results for the Weineisen test are shown in his paper’s Figures 5-6. Our comparisons will be with Figure 5, reproduced here as Fig. 6, which shows the time histories of several quantities:

1. The simulated absolute moisture volume (cc) decreases nearly linearly until 1.8s then decreases more slowly until it reaches zero at 2.54s. The net drying time, 2.54s, is in good agreement with the experimental data, Fig. 7. When compared with the data, however, the computed moisture content at 1s is $1/2$ the initial value, while in the measured data the moisture content is $1/3$. The computed drying rate is nearly constant for 2s and then tapers to zero over the remaining 0.5s. Measurements, in contrast, show a faster drying rate over the first 1.0s and then a slower rate over the remaining 1.5s. What is peculiar about the measurements is that the flow velocity reaches its maximum value when there is still a significant amount of moisture in the paper ($1.0\text{kg}/\text{kg}$ or $1/3$ the initial amount). It is expected that the flow rate should increase as moisture is removed (i.e., with increasing porosity) and this is true in the simulation.
2. The computed airflow velocity upstream of the paper, Fig. 8, has the same qualitative shape as the measurements. There is a ramp up of velocity during the

first 2.5s followed by a constant velocity after all the moisture has been evaporated, but the values during the first 2.1s are lower than the measured values by about half. Both the measured and computed velocity after drying are the same (about 250cm/s), which is not surprising since this was how the permeability for the simulation was determined.

- Weineisen's measured humidity, lower right plot in Fig. 6, shows a peak value around 0.05kg/kg at about a time of 0.2-0.3s. The simulated peak occurs at 0.2s and has a somewhat lower value of 0.03kg/kg, but otherwise has the same qualitative shape.

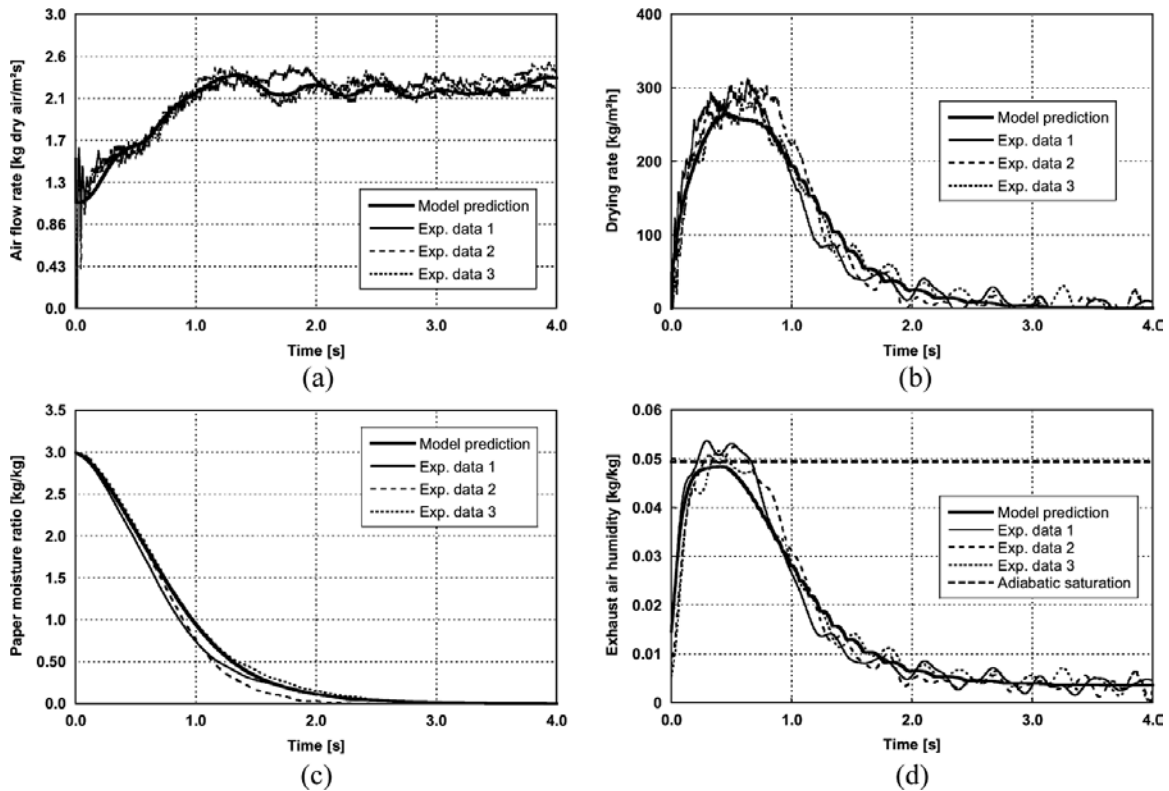


Figure 6. A reproduction of Figure 5 from Weineisen's paper.

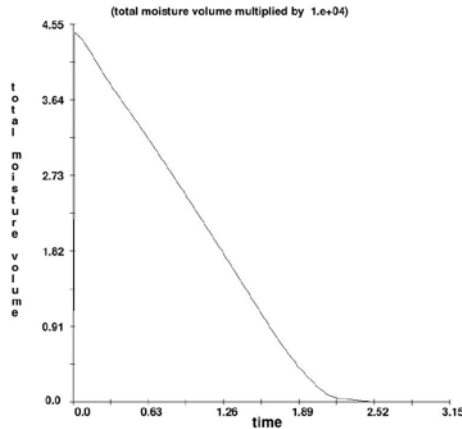


Figure 7. Moisture volume vs. time.

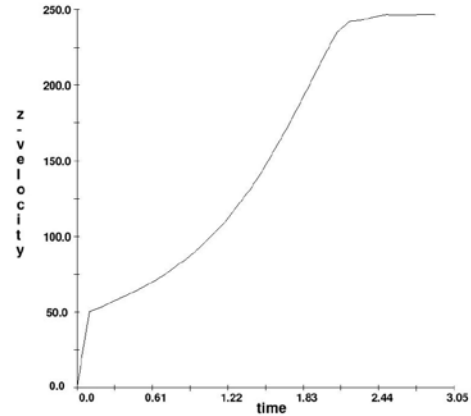


Figure 8. Upstream velocity vs. time.

4. At 0.2s, in the last paper layer downstream, the gas temperature is 351°K while the moisture temperature is 302.5°K. The simulated vapor pressure in this layer is $p= 4.7e+4$ dynes/cm², which is close to the saturated vapor pressure corresponding to the moisture temperature, $p=4.3e+4$ dynes/cm². The computed value is slightly higher than the saturated value based on the moisture temperature, which may be because of the higher air temperature heating the vapor, or some other non-equilibrium process. It should also be remarked that in the program the output for “saturated vapor pressure” is a value computed from the temperature of the gas. In the interior of the drying paper, however, it is the moisture/solid (water/fiber) temperature that controls the local saturation state (i.e., whether there is condensation or evaporation). Even though the air is warm enough to contain more vapor, the moisture in the paper cannot evaporate beyond the saturation level corresponding to its temperature. In this sense, the simulation does agree with the experimental observation that the gas leaving the downstream side of the paper is nearly saturated.

Discussion

Application of the new drying model to an experimental test conducted by Weineisen and Stenström has produced results that are in good qualitative agreement with the data. Good quantitative agreement exists for the total drying time, the condition of nearly saturated flow leaving the paper during drying and the flow rate through dry paper.

Overall, the agreement seems satisfactory in view of what appears to be some inconsistency in the data. For example, the flow velocity reaching its maximum value while there is still a considerable amount of moisture in the paper.

The weakest element of the simulation is the determination of the permeability. Could it be that the inertial (i.e., quadratic velocity) portion of the permeability is playing a larger role in this test problem than it did in the first test case? An evaluation of the ratio of the inertial portion versus the viscous portion of the permeability shows that this is not the case. The inertial part is about three orders of magnitude smaller than the viscous part, even at the largest flow velocity observed in the test. In general, if the fibers in the paper

are small enough, the inertial versus viscous contribution to permeability will always be small.

Summary

A new model for numerically simulating the through-air drying of paper has been developed and partially validated against experimental data. The expression “partially validated” is used because little data was found to perform validation tests. This is especially true of drying conditions at high moisture contents, high flow through rates and air temperatures much higher than room temperature.

Appendix: Input file for Weineisen Test Problem

```
Test paper drying using pressure drop -- Weineisen data
&xput
  remark='units are cgs-degrees K',
  twfin=3.0, deltt=1.0e-6, pltdt=0.1,
  itb=0,
  nmat=2, icmprs=1,
  ifvisc=1,
  ifenrg=2, imphtc=1,
  ihtc=2,
  idrg=4,
  epsadj=1.0,
  iadix=0,
  incg=1, remark='activate non-condensable gas',
  iphchg=6, remark='activate moisture phase change',
/

&limits
  itmax=200, itflmx=25, itdtmx=25, itvsmx=20,
  mrstrt=10, ncflmx=4,
/

&props
  remark='fluid2 is water vapor with non-condensable air',
  rhof=1.0, rhof2=3.0e-5, mu2=1.7e-4,
  cv2=1.14e+7, rf2=4.55e+6, remark='rf2=(gamma-1)*cv2',
  thc2=3000.0,
  cvnc=7.18e+6, rfnc=2.78e+6,
  rsize=0.01,
  pv1=3.5814e+6, tv1=413.0, tvexp=2.0e-4,
  remark='sat-props from table',
/

&scalar
  iphchm=1,
/

&bcddata
  wl=1, wr=1,
  wf=1, wbk=1,
  wb=5,
  pbct(1,5)=1.0233e+6, remark='1.01325e+6',
```

```

fbct(1,5)=0.0,  tbct(1,5)=423.0,  remark='301.3=28.3C',
wt=5,  pbct(1,6)=1013250.0,  fbct(1,6)=0.0,  tbct(1,6)=423.0,
cncbc(5)=0.9996,  cncbc(6)=0.9996,
/

&mesh
  nxcelt=16,  px(1)=0.0,  px(2)=0.2,
  nycelt=1,  py(1)=0.0,  py(2)=1.0,
  nzcelt=30,  pz(1)=0.8,  pz(2)=1.075,  pz(3)=1.096,  pz(4)=1.3,
  nzcell(2)=6,
/

&obs
  avrck=-3.1,
  nobs=1,
  iob(1)=1,  remark='paper',
  twobs(1,1)=301.3,  kobs(1)=1.26e+4,
  rcobs(1)=0.6e+7,  hobs2(1)=3.0e+4,
  oadrg(1)=9.18e+8,  obdrg(1)=4548.0,  remark='d=0.0016cm',
  opor(1)=0.91,  ospor(1)=204.0,
  remark='guessing Rod PoreSize=0.0021',
  obsm(1)=0.107,  obsmrc(1)=4.187e+7,
  obsmrl(1)=2.26e+10,  remark='not needed obsmt(1)=373.0',
  zl(1)=1.075,  zh(1)=1.096,
/

&fl
  presi=1013250.0,
  flht=-1.0,
  cnci=0.9996,  remark='initial air content',
/

&bf
  nbafs=1,
  remark='fabric support mesh - approx. Weineisen equ.12',
  bz(1)=1.096,  pbaf(1)=0.9,  kbaf2(1)=0.0346,
/

&temp
  tempi=301.3,
/

&motn
/

&grafic
/

&HEADER
  PROJECT='PaperVal_Weineisen',
/

&parts
/
  "A Model for Through Drying of Tissue Paper at Constant Pressure
  Drop and High Drying Intensity," H.Weineisen and S. Stenstrom,
  Drying Tech. 25, 1949-1958, (2007).

```

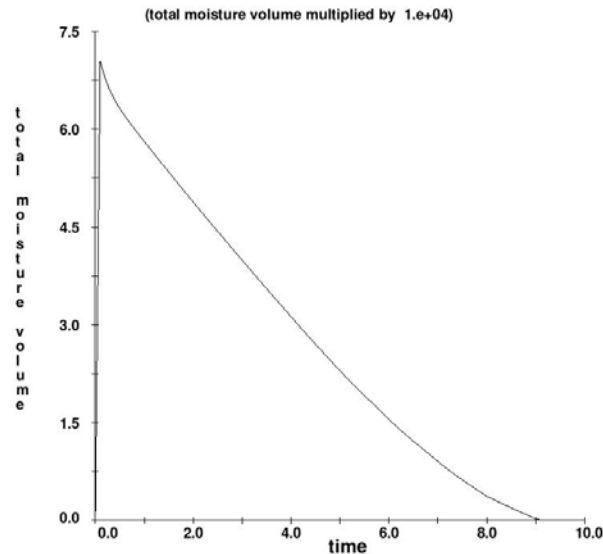


Figure 6. Total moisture content as a function of time.

Nevertheless, the model has been constructed on basic physical principals and is similar to other phase-change models that have proven to be reliable. For these reasons it is believed that the model will provide significant and useful results. Further testing may reveal the need for some adjustment in the permeability versus moisture relation, but this should be a relatively easy adjustment to make.

References

- [1] Polat, O. "Through Drying of Paper," Ph.D. dissertation. Dept. Chem. Eng., McGill Uni., Montreal, Canada (1989).
- [2] Bear, J., "Dynamics of Fluids in Porous Media," Dover Pub., N.Y., (1972).
- [3] Ryan, M., Zhang, J. and Ramaswamy, S., "Experimental Investigation of Through Air Drying of Tissue and Towel under Commercial Conditions," Drying Tech. **26**, 195 (2007).

Appendix

The prepin.inp file used for the validation problem contains a complete list of physical and numerical parameters used by the simulation, as well as the program options that are needed to perform the simulation.

```
Test paper drying using specified flow rate -- Ryan data
&xput
  remark='units are cgs-degrees K',
  twfin=10.0, delt=1.0e-6, pltdt=0.1,
  itb=0,
  nmat=2, icmprs=1,
  ifvisc=1,
  ifenrg=2, imphtc=1,
```



```

    ihtc=2,
    idrg=4,
    epsadj=1.0,
    iadix=0,
    incg=1,    remark='activate non-condensable gas',
    iphchg=6,  remark='activate moisture phase change',
/
&limits
    itmax=200, itflmx=25, itdtmx=25, itvsmx=20,
    mrstrt=10, ncflmx=4,
/
&props
    remark='fluid2 is water vapor with non-condensable air',
    rhof=1.0,  rhof2=3.0e-5,  mu2=1.7e-4,
    cv2=1.14e+7,  rf2=4.55e+6, remark='rf2=(gamma-1)*cv2',
    thc2=3000.0,
    cvnc=7.18e+6,  rfnc=2.78e+6,
    rsize=0.01,
    pv1=4.1950e+4,  tv1=303.0,  tvexp=2.0e-4, remark='sat-props from
table',
/
&scalar
    iphchm=1,
/
&bcdata
    wl=1,  wr=1,
    wf=1,  wbk=1,
    wb=6,  wbct(1, 5)=45.4,  remark='specified flow rate',
    pbct(1,5)=1.026e+6, remark='1.01325e+6',
    fbct(1,5)=0.0,  tbct(1,5)=296.3, remark='301.3=28.3C',
    wt=5,  pbct(1,6)=1013250.0, fbct(1,6)=0.0,  tbct(1,6)=301.3,
    cncbc(5)=0.9996,  cncbc(6)=0.9996,
/
&mesh
    nxcelt=16,  px(1)=0.0,  px(2)=0.2,
    nycelt=1,   py(1)=0.0,  py(2)=1.0,
    nzcelt=30,  pz(1)=0.8,  pz(2)=1.075, pz(3)=1.1,  pz(4)=1.3,
                    nzcell(2)=6,
/
&obs
    avrck=-3.1,
    nob=1,
    iob(1)=1, remark='paper',
    twobs(1,1)=301.3, kobs(1)=1.26e+4,
    rcobs(1)=0.6e+7,  hobs2(1)=3.0e+4,
    oadrg(1)=4.5e+9,  obdrg(1)=10000.0, remark='d=0.0002cm',
    opor(1)=0.90,  ospor(1)=490.0,  obsm(1)=0.147,  obsmrc(1)=4.187e+7,
    obsmrl(1)=2.26e+10,  obsmt(1)=373.0,
    zl(1)=1.075,  zh(1)=1.1,
/
&fl
    presi=1013250.0,
    flht=-1.0,
    cnci=0.9996,  remark='initial air content',
/
&bf
    nbafs=0,  remark='honeycomb support mesh',

```

```
    bz(1)=1.1, pbaf(1)=0.9, kbaf2(1)=0.123,
    remark='area fraction combines with paper fraction, could set
pbaf=0'
    remark='loss is small in any case so ignoring support mesh',
/
&temp
    tempi=301.3,
/
&motn
/
&grafic
/
&HEADER
    PROJECT='PaperVal_Ryan3',
/
&parts
/
    "Experimental Investigation of Through Air Drying of Tissue and
Towel under commercial Conditions," by Matthew Ryan, Jiehai Zhang and
Shri Ramaswamy, Drying Technology, 25, p195-204, 2007.
```